



PERSISTENT CURRENT FIELDS IN FERMILAB TEVATRON MAGNETS*†

B. C. Brown, H. E. Fisk, and R. Hanft

May 1985

*An abbreviated version of this paper is published in IEEE Trans. on Magnetics MAG-21, 979, 1985.

†Submitted to the Proceedings of the 1984 Applied Superconductivity Conference, September 10-13, 1984, San Diego, California.



Persistent Current Fields in Fermilab Tevatron Magnets

B. C. Brown, M. E. Pisk, and R. Hanft

Fermilab National Accelerator Laboratory*
P.O. Box 500
Batavia, Illinois 60510

Abstract

Data on the persistent current residual fields in Tevatron dipoles and quadrupoles are presented. The data are compared to the doublet theory of persistent current fields and an estimate is given for the multipole fields expected in the Superconducting Super Collider (SSC) dipole proposed by Fermilab.

Introduction

The magnetization that is generated by currents due to the Meissner effect in type II superconducting filaments has been experimentally observed in many accelerator and beam line magnets^{1,2,3} and a doublet theory has been developed that accounts for the gross features of the resultant persistent current fields.⁴ The dipole and sextupole fields, for 3 in. to 5 in. bore diameter dipoles at a reference radius of 2/3 the aperture, are typically of the order of 10 gauss. A persistent dipole field of this magnitude is not a problem for accelerator performance since it does not affect the machine's dynamic aperture. However, the effect of the persistent sextupole field is to produce disastrous chromatic aberrations at low magnet excitation (injection, for example) that must be corrected if the accelerator is to perform over a large dynamic range, say 20 to 1, as anticipated in the SSC reference design.⁵ Although there may be straightforward ways to compensate the unwanted sextupole and higher multipoles with individual magnet correction coils it may be possible to improve on the fundamental dipole design and incorporate the corrections in the magnet at the construction stage. This later possibility will require a thorough understanding of the mechanism whereby persistent fields are generated. It is in this spirit that the data and calculations on Fermilab Tevatron magnets are presented.

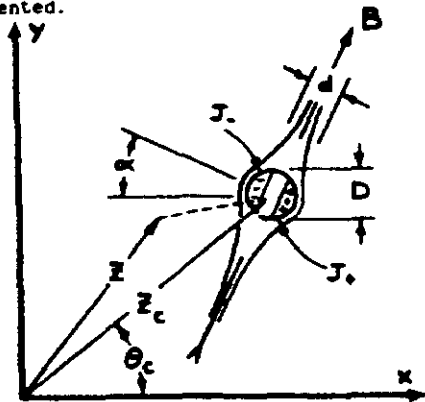


Figure 1 Superconducting filament of diameter D in an external magnetic field B. The center of the filament is located at z_c and the field point is z . The induced current elements I^+ and I^- are separated by distance d . The angle α subtends the line between the centers of induced current and the x axis.

*Operated by Universities Research Assn. Inc., under contract with the U.S. Department of Energy.

An abbreviated version of this paper is published in IEEE Trans on Magnetics MAG-21, 979, 1985. Proceedings of 1984 Applied Superconductivity Conference.

Theory

Figure 1 shows a superconducting filament in an external field and the Meissner effect induced persistent (shielding) currents that give rise to the residual field. As discussed in the papers by Green^{1,2}, the complex field $B' = B' + iB''$ at the observation point z , due to a filament at z_c is:

$$B'_y + iB'_x = \frac{-\mu_0 I_0 e^{i\alpha}}{2\pi(z-z_c)^2} \quad (1)$$

The doublet strength, Γ , is the average $I d$ where d is the distance between the positive and negative current elements and I is the integrated current densities J^2 over the region of penetration. The value of Γ depends on the previous magnetic history of the superconductor, filament diameter D , and the critical current density $J_c(B)$ at the local filament site. The angle α is perpendicular to the B field that is external to the filament and gives the orientation of the current doublet.

To find the persistent current multipole moments for magnets with dipole symmetry, i.e., $J(-z) = -J(z)$, the expression given above is expanded in powers of z/z_c and integrated:

$$b'_n = \frac{\mu_0(n+1)}{\pi} \int \Gamma'(D, J_c, J_t) r_c^{-n-2} \cos[(n+2)\theta_c - \alpha] dA \quad (2)$$

with $n=0,2,4$, for dipole, sextupole, decapole normal moments. For quadrupole magnets there is an analogous expression. The persistent current field is expressed in the power series:

$$B'_y + iB'_x = \sum_{n=0} c'_n z^n; \quad c'_n = b'_n + ia'_n \quad (3)$$

and $z = x + iy$. For dipole symmetry all the persistent skew moments, a'_n , vanish. If, for example, the top and bottom dipole coils are made from superconductor whose J_c vs B curves are different, then persistent current skew moments may appear in measured data. The factor Γ' is $\Gamma \rho$ where ρ is the area density of filaments. Γ' also includes a factor that accounts for the transport current density, J_t . For the simplified model in Figure 1,

$$\Gamma' = \frac{2\epsilon D J_c(B) [1 - J_t/J_c(B)] \beta}{(1+\alpha)} \quad (4)$$

Here ϵ is the doublet strength factor which depends on the depth of penetration of the persistent currents within the filament. For a fully penetrated filament the model of M. A. Green gives $\epsilon = 0.423$. The critical current density J_c , the coil packing factor β , i.e. the fraction of the area that is metallic, and the area ratio of copper to superconductor, α , also appear in the expression for Γ' . It should be noted that, other factors being equal, the persistent current fields are proportional to the filament diameter, D . In comparing persistent fields generated in magnets with similar geometry but different filament size the parameter, ϵ , that describes the extent of penetration must be known.

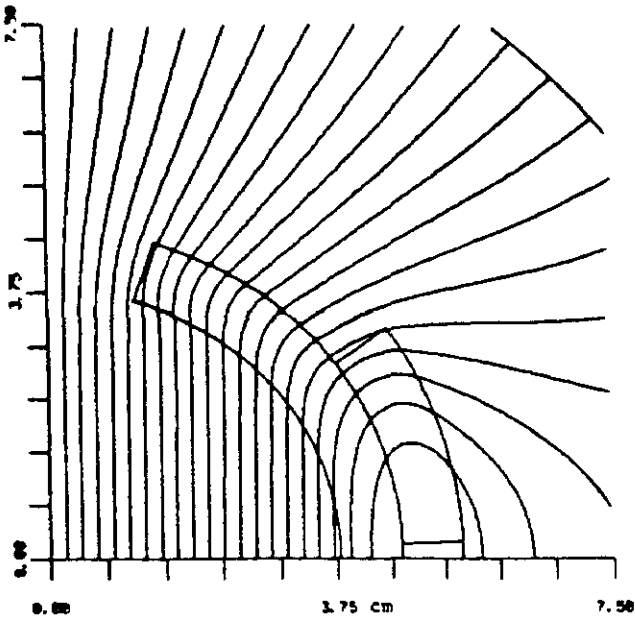


Figure 2 Tevatron dipole coil cross section and magnetic field.

This is particularly true in the low current region where the filaments are not fully penetrated by the shielding currents. An estimate of the penetration depth, δ , is obtained by applying $\nabla \times \vec{B} = \mu_0 \vec{J}$ at the edge of a filament. The change in B necessary to achieve full penetration is found from $\delta = \Delta B / \mu_0 J_c$. For J_c of 12×10^9 A/m² and filaments of $10 \mu\text{m}$, a flux change of about 1kG is sufficient to saturate the filaments with shielding current.

To calculate the persistent fields a transport current magnetic field map is generated with one of the standard field calculation programs. As an example the Tevatron dipole winding and field are shown in Figure 2. When the field is known inside the winding the values of J_c and a can be determined and the integral in equation (2) can be performed. The critical current density, J_c , for NbTi as a function of B is given in the paper of Green.² It should be noted that there can be considerable variation in J_c which in turn leads to uncertainty in calculated residual fields especially at low currents.

Data

Measurement Technique

The data on persistent fields have been obtained by integrating the output voltage of a rotatable flat measuring coil designed specifically for accurate measurement of the multipole fields of Tevatron dipoles and quadrupoles.³ The measuring coils are fabricated with bucking coils so that the dominant fields are reduced to the point where the other multipoles can be easily measured. Fourier analysis of the resultant signal, along with the known geometry of the measuring coils, yields the various harmonic coefficients in the multipole expansion

$$B_y + iB_x = B_0 \sum_{n=0}^{\infty} c_n z^n ; c_n = b_n + ia_n$$

where b_n, a_n are sums of contributions from the transport current and the persistent current. These coefficients are reported at a reference radius of 1

in standard units, where a standard unit is obtained by suppressing a factor of 10^{-4} and B_0 is the main field (the dipole field for dipoles or the quadrupole field for quadrupole magnets). This technique obtains coefficients to an absolute accuracy of 0.5 unit and to a relative accuracy of 0.1 unit for measurements made sequentially at different magnet excitations. In Tevatron magnets there is almost no variation in b_n, a_n with magnet excitation ascribable to iron saturation⁴ in the yoke or coil deformation, and we interpret observed variation in b_n to be due to variation in b'_n .

Not only must a reliable measurement of the harmonic components of the magnetic field be made, but also the power supply that provides the transport current must make transitions from one current level to the next without overshoot(undershoot) as the current is increased(decreased). The latter is essential because of the hysteretic behavior of the superconductor as the data presented here will show.

Quadrupole Data

Figure 3 shows the 12-pole moment, b_{12} , hysteresis curves for two Tevatron quadrupoles with the same geometrical cross-sections but different filament size wire. The data for the standard quadrupole (-9 μm filaments) are labeled TQ122D while the other set is obtained from measurements on a low beta insertion quadrupole Q1402 (-19 μm filaments). The ratios of the measured differences $R = \Delta b_{12}(\text{std cable}) / \Delta b_{12}(\text{low beta cable})$ at 300, 400, 500 and 600A are 0.36, 0.39, 0.37, and 0.40, respectively. The average of these values is 0.38. To compare these results with the prediction of the persistent current theory we note that expressions (2) and (4) differ only in the factor $cD/(1+s)$ for magnets with identical geometry but different wire.

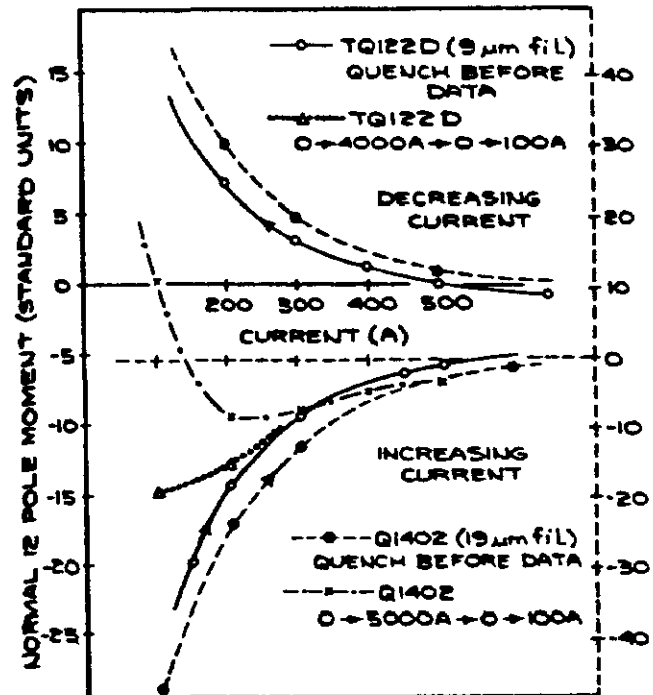


Figure 3 Tevatron quadrupole 12 pole moment b_{12} vs current. The scales on the left and right refer to the standard quadrupole TQ122D(9 μm filaments) and the low beta insertion quadrupole Q1402(19 μm filaments), respectively.

If ϵ is assumed to be the same for both magnets and the quantity $(1+\epsilon)$ can be recast in terms of the number of filaments and their cross sectional areas, then we obtain the theoretical ratio

$$R_{th} = \frac{2050 D^2(\text{std cable})}{510 D^2(\text{low beta cable})}$$

The number of filaments in the standard and low beta strands is, respectively, 2050 and 510. The theoretical ratio with the nominal filament diameters of 8.7 and 19.3 μm is 0.37 which is in good agreement with the measured data. Comparison of the 12 pole hysteresis data and a theoretical calculation for 9 μm filaments shows agreement at the 15 to 20% level. For example, at 300A the measured and calculated values of B_2 are -0.86g and -1.03g, respectively. The calculations also indicate that for the current region above 300A one need not worry about the relative penetration in the two different cables, i.e. the ratio of 12 pole moments from quads built with the two different filament size cables needs to be corrected by less than 10% in the 300 to 600A region.

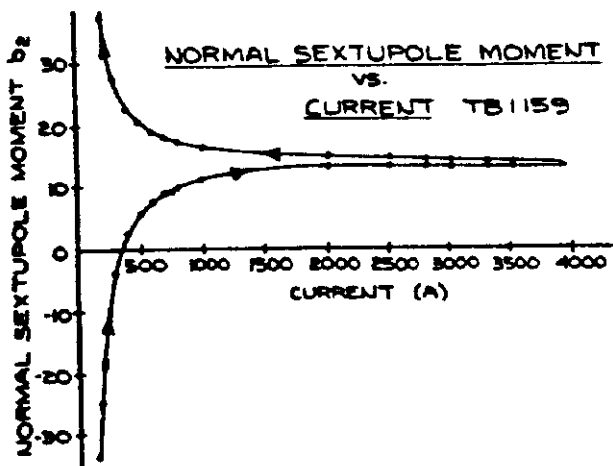


Figure 4 Normal sextupole moment b_2 vs. current for Tevatron dipole TB1159.

Dipole Data

In the routine measurements of Tevatron dipoles and quadrupoles, harmonic data were not usually taken for currents below 660A which corresponds to the injection field for the Tevatron. Recently a few dipoles have been measured to determine the current dependence of the residual fields. Figure 4 shows the variation with current of the normal sextupole moment, b_2 , for the central longitudinal portion of TB1159 which had been quenched before the displayed data were taken. Each point on the graph was obtained with the magnet current held constant while the measuring probe was slowly rotated to obtain the multipole data. A negative sextupole moment was observed at low excitation, which then increased as the magnet current was increased. At 4000A the current was reversed (down ramp) and data were again accumulated. The difference, $\Delta b_2 = b_2(\text{down ramp}) - b_2(\text{up ramp})$ at a fixed current, depends on the product $J \cdot D$. Thus, the large value of Δb_2 at low current is primarily due to the increased value of J , as, B , the field in the winding, is decreased. For magnet TB1159, Δb_2 at 1000A is 5 units. A histogram of Δb_2 at 660A for Tevatron dipoles shows an rms

variation of about 10%. This represents the J variation in manufacture of the wire and is consistent with the measured short sample data at 5T¹⁰.

The asymptotic value of the normal sextupole moment, b_2 , for TB1159 is 13.7 units, which is close to the average of 13.4 units for the center portion of Tevatron dipoles. The central 13.4 units are used to balance the negative sextupole generated by the ends of the winding. To find the persistent current sextupole in gauss, we calculate $B_2 = B_0 r^2 (b_2 - b_2^0)$ at $r = 1$ in. The current dependence of B_2 is indicated in Figure 5. Data from two different up ramps show a one gauss difference at 80A depending on whether the magnet has been quenched before the data were taken. The sextupole field at 220A is -6 gauss at 1 in. A calculation of the expected persistent current sextupole field is also given. Although the theoretical curve is not a good fit to the data, the level of persistent field is correct in the region of interest and gives confidence that different dipole geometries, such as those of interest for the SSC, can be reasonably reckoned.

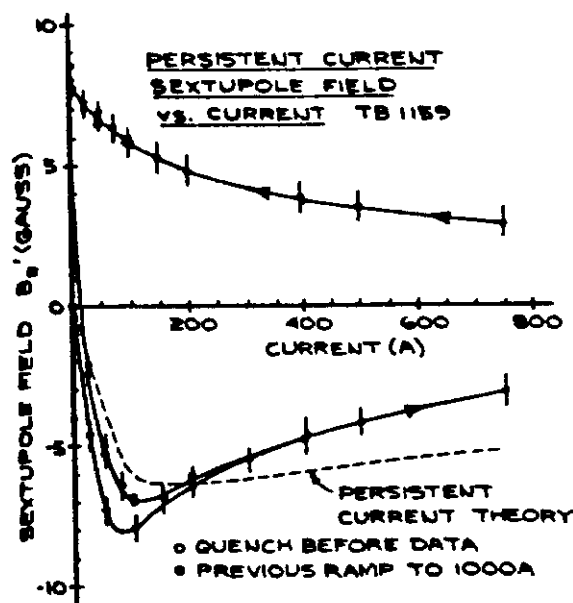


Figure 5 Current dependence of the Tevatron dipole persistent sextupole field at $r=1$ in. The sextupole moment due to the geometric placement of conductor has been subtracted from the measured data to yield the plotted points. See text.

Figure 6 shows the average normal decapole moment data with increasing current for dipoles TB0459 and TB1159. Displayed in the inset is the normal decapole field in gauss. The expected theoretical curve is also shown. Note that the decapole field drops off much more rapidly than the sextupole field. Again the shape of the theoretical curve is not a good representation of the data, but the sign and magnitude (+1 gauss) of the calculation agree well with the measured data.

The persistent current also generates a dipole field that is predicted to be -5 gauss at 300A for increasing current, while the value after an up and down cycle ending at zero current is predicted to be

about 7 gauss. By cycling the magnet and then measuring the dipole field after the power supply has been shut down, the residual dipole can be measured. Care must be taken to also determine the field due to the iron yoke that surrounds the cryostat. To measure the remanent iron field, it is necessary to annihilate the superconducting persistent currents by warming the superconductor either (1) by quenching the magnet on a second ramp that follows the residual field measurement, or (2) by flowing warm gas through the magnet until its temperature is above 10K. Both methods yield 6 ± 0.5 gauss for the iron field; and when this is subtracted from the residual field, the result is 6.9 and 7.1 gauss for the persistent dipole fields in magnets TB0409 and TB1159, respectively. Current dependent measurements have also been made with an NMR probe that has the sensitivity to measure absolute fields to better than 1 gauss. By subtracting the up and down ramp NMR data at 1000A a difference of -14 gauss is obtained as anticipated.

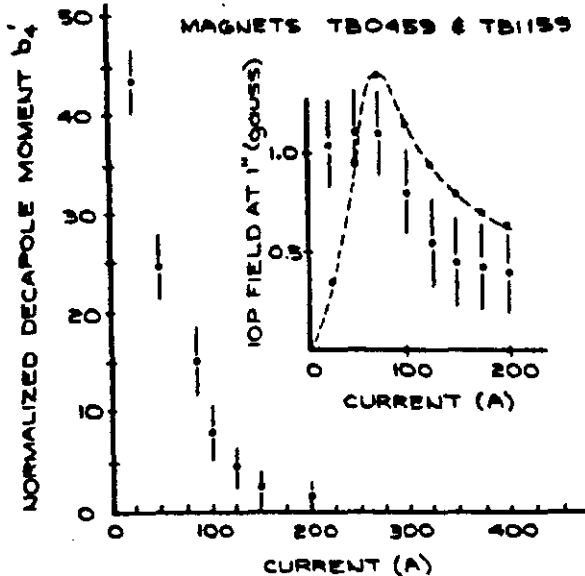


Figure 6 Dipole magnet persistent decapole moment b_4 vs. current. The inset shows the decapole field in gauss and the theoretical prediction (dashed curve).

Transition Curves

Figure 7a shows some sextupole moment data from TB0409 taken in a manner similar to TB1159 data shown in Figure 4. Also shown is the hysteresis that results when the down ramp is halted at 400A and the current is reversed. Such a transition shows that after a ΔI of 300A, when the current is 700A, the filaments are saturated with the reverse persistent current and the persistent sextupole field is nearly the same as when the winding was excited without previous magnetic history. Similar data obtained after a different current reversal point, e.g. 1000A, show similar behavior.

If Δb_2^t is the difference between the down ramp data and the transition curve, then the quantity $\Delta b_2^t / \Delta b_2$ is a normalized measure of filament penetration since Δb_2 measures cJ and Δb_2 is proportional to J ; see equations (2) and (4). Transition curve data from Figure 7a is replotted in Figure 7b as $\Delta b_2^t / \Delta b_2$ versus $\Delta I = I(\text{current reversal}) - I$. Figure 7b also shows the normalized filament penetration versus a scaled ΔI for the 1000A transition curve: Previously it was indicated that δ is approximately equal to $\Delta B / \mu_0 J_c$; and since ΔB is

proportional to ΔI , the universality of transition curves can be measured by scaling ΔI with J_c . Since the average value of J_c is 25% higher in the 400A region than in the 1000A to 1200A region, the normalized transition curve data with current reversal at 1000A are plotted against $\Delta I^{1.25}$. The universality of transition curves is clearly indicated.

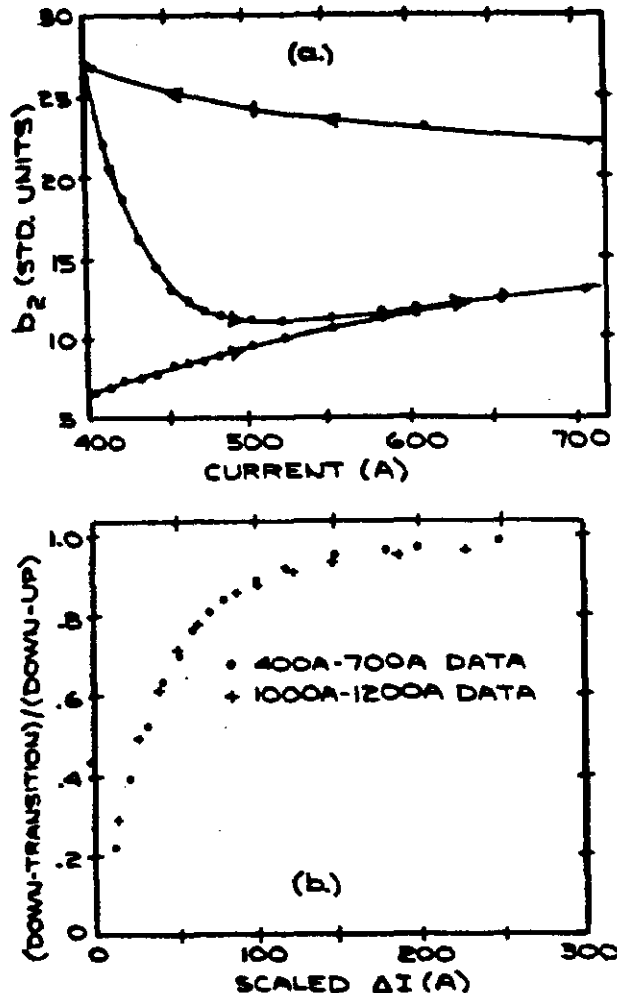


Figure 7(a) TB0409 normal sextupole moment, b_2 , vs. current; the transition curve shows how b_2 changes when the down ramp is halted at 400A and the current is reversed. (b) Variation of the scaled b_2 vs. scaled current. Scaled data from two transition curves are plotted.

SSC Dipole

The proposed 2 in. diameter aperture Fermilab version of the SSC dipole has a two shell coil with wedges in the coil winding to provide field shaping. The inner shell conductor cable is made from 0.030 in. diameter strands containing 710 Nb47.5%Ti filaments of diameter 16.5 μ m. While the proposed outer shell has somewhat less superconductor, calculations on persistent fields have assumed the same conductor in both shells. The current dependence of the persistent dipole, sextupole, and decapole is expected to be very similar to the

measured data just discussed. A computer calculation gives the following fields (B_1 , B_2 , B_3) at 5%, 10%, and 15% of full field (5T) and at a reference radius of 2/3 the aperture: (-10.5g, -10.3g, 1.6g), (-9.2g, -9.2g, 0.9g), and (-8.1g, -8.1g, 0.7g), respectively. These fields can be halved by using smaller filaments, but even then there will need to be persistent current field correction elements unless steps are taken at the magnet design level to reduce these fields. Two possible schemes using, (a) filament size variation in the winding or (b) use of passive superconductor, have been suggested as ways to get around this problem.¹¹

References

1. M. A. Green, Residual Fields in Superconducting Dipole and Quadrupole Magnets, UCRL-20171 or IEEE Trans. on Nucl. Sci. NS-18 (3)pp664-668(1971).
2. M. A. Green, Fields Generated within the SSC Magnets due to Persistent Currents in the Superconductor, Proc. of the Workshop on Accelerator Physics Issues for a Superconducting Super Collider, M. Tigner (Ed.)pp126-131(1983); (see references therein) Univ. of Michigan, Ann Arbor, Michigan.
3. E. Bleser et al. Measurement of Magnetization Effects in CBA Magnets; Proc. of the Workshop on Accelerator Physics Issues for a Superconducting Super Collider, M. Tigner (Ed.)p95(1983) Univ. of Michigan, Ann Arbor, Michigan.
4. M. A. Green, Residual Fields in Superconducting Magnets, Proc. of the Magnet Technology Conference MT-4 p339(1972). Brookhaven National Laboratory.
5. Superconducting Super Collider; Reference Designs Study for the U.S. Department of Energy, May 8, 1984, p94 (unpublished).
6. R. A. Beth, Proc. of the 6th Int'l. Conference on High Energy Accelerators, Ed. R. A. Mack, C.E.A., p387(1967) Cambridge, Mass.
7. R. A. Beth, J. appl. Phys. 37 2568(1966).
8. K. Halbach, Nucl. Inst. and Meth. 78 185-198 (1970).
9. B. C. Brown et al, "Report on the Production Magnet Measurement System for the Fermilab Energy Saver Superconducting Dipoles and Quadrupoles". IEEE Trans. on Nucl. Sci. NS-30 3608(1983).
10. A. D. McInturff et al, Paper LL-5, this conference.
11. B. C. Brown and H. E. Fisk, A Technique to Minimize Persistent Current Multipoles in Superconducting Accelerator Magnets, to be published in Proc. of the 1984 Summer Study on the Design and Utilization of the Superconducting Super Collider.